Trim32 reduces PI3K–Akt–FoxO signaling in muscle atrophy by promoting plakoglobin–PI3K dissociation

Trim32 reduces PI3K–Akt–FoxO signaling in muscle atrophy by promoting plakoglobin–PI3K dissociation

Shenhav Cohen, Donghoon Lee, Bo Zhai, Steven P. Gygi, and Alfred L. Goldberg

Department of Cell Biology, Harvard Medical School, Boston, MA 02115

Activation of the PI3K–Akt–FoxO pathway induces cell growth, whereas its inhibition reduces cell survival and, in muscle, causes atrophy. Here, we report a novel mechanism that suppresses PI3K–Akt–FoxO signaling. Although skeletal muscle lacks desmosomes, it contains multiple desmosomal components, including plakoglobin. In normal muscle plakoglobin binds the insulin receptor and PI3K subunit p85 and promotes PI3K–Akt–FoxO signaling. During atrophy, however, its interaction with PI3K–p85 is reduced by the ubiquitin ligase Trim32 (tripartite motif containing protein 32). Inhibition of Trim32 enhanced plakoglobin binding to PI3K–p85 and promoted PI3K–Akt–FoxO signaling. Surprisingly, plakoglobin overexpression alone enhanced PI3K–Akt–FoxO signaling. Furthermore, Trim32 inhibition in normal muscle increased PI3K–Akt–FoxO signaling, enhanced glucose uptake, and induced fiber growth, whereas plakoglobin down-regulation reduced PI3K–Akt–FoxO signaling, decreased glucose uptake, and caused atrophy. Thus, by promoting plakoglobin–PI3K dissociation, Trim32 reduces PI3K–Akt–FoxO signaling in normal and atrophying muscle. This mechanism probably contributes to insulin resistance during fasting and catabolic diseases and perhaps to the myopathies and cardiomyopathies seen with Trim32 and plakoglobin mutations.

Introduction

Growth of skeletal and cardiac muscles, like that of dividing cells, is largely dependent on signaling through the insulin–PI3K–Akt–FoxO pathway. Conversely, the atrophy of specific muscles upon disuse or denervation and the systemic muscle wasting in fasting and disease states (e.g., cancer cachexia, sepsis, and untreated diabetes) results from reduced activity of this pathway (Stitt et al., 2004; Glass, 2010). This rapid loss of muscle mass results primarily from the accelerated degradation of myofibrillar and soluble proteins, but in most catabolic states (e.g., fasting), protein synthesis also decreases.

Development of these various types of atrophy requires the transcription of a common set of atrophy-related genes ("atrogenes"; Lecker et al., 2004) by FoxO transcription factors, whose activation is sufficient to cause accelerated proteolysis and atrophy (Sandri et al., 2004). In atrophying muscles, multiple components of the ubiquitin-proteasome pathway, such as the muscle-specific ubiquitin ligases muscle RING-finger 1 (MuRF1) and Atrogin1/MAFbx (Bodine et al., 2001; Gomes et al., 2001), are induced, and their induction is essential for rapid wasting. Another ubiquitin ligase that appears to be critical for atrophy is Trim32 (tripartite motif containing protein 32; Cohen et al., 2012). Like MuRF1, Trim32 contains a tripartite motif (RING; B-box; coiled-coil), but also has six NHL repeats with putative protein-binding properties (Slack and Ruvkun, 1998; Frosk et al., 2002), and mutations in the third repeat cause limb girdle muscular dystrophy 2H (LGMD-2H). We demonstrated that during muscle wasting, MuRF1 is essential for the ubiquitin-dependent degradation of proteins comprising the thick filament (Cohen et al., 2009), whereas Trim32 catalyzes the disassembly and degradation of the desmin cytoskeleton, Z-band, and thin-filament proteins, which are linked processes (Cohen et al., 2012). Surprisingly, the down-regulation of Trim32 in muscle reduced not only the breakdown of these contractile and cytoskeletal proteins, but also the total loss of muscle mass upon fasting (Cohen et al., 2012). Therefore, Trim32 must have other critical substrates in muscle that accumulate upon Trim32 inhibition and block protein breakdown and/or promote protein

Correspondence to Alfred L. Goldberg: alfred_goldberg@hms.harvard.edu

Abbreviations used in this paper: DN, dominant negative; MuRF1, muscle RING-finger 1; TA, tibialis anterior; Trim32, tripartite motif containing protein 32.

The Rockefeller University Press $30.00
J. Cell Biol. Vol. 204 No. 5 747–758
www.jcb.org/cgi/doi/10.1083/jcb.201304167

synthesis and growth. The present studies were undertaken to test this intriguing hypothesis and to identify the proposed growth-regulatory factor whose function is controlled by Trim32.

These studies have identified a novel protein in skeletal muscle, plakoglobin, whose function is regulated by Trim32. Plakoglobin is a component of the desmosome adhesion complex that is prominent in tissues that must withstand mechanical stress, especially cardiomyocytes and epithelia (Buxton et al., 1993; Koch and Franke, 1994; Gumbiner, 1996, 2005). In epithelia, plakoglobin regulates signaling pathways (e.g., by Wnt) that control cell motility (Jamora and Fuchs, 2002), growth, and differentiation (Calautti et al., 2005). We show here that plakoglobin is of prime importance in regulating muscle size because it binds to the insulin receptor and enhances the activity of the PI3K–Akt–FoxO pathway. Activation of this pathway by IGF-I or insulin promotes overall protein synthesis and inhibits protein degradation (Sacheck et al., 2004; Glass, 2005) by both autophagy and the ubiquitin-proteasome pathway (Mammucari et al., 2007; Zhao et al., 2007). During fasting and in disease states, when IGF-I and insulin levels are low, PI3K–Akt–FoxO signaling decreases, and proteolysis increases largely via FoxO-mediated expression of the atrogene program (Sandri et al., 2004). Also, in untreated diabetes, sepsis, and cancer cachexia (Zhou et al., 2010), impaired signaling through this pathway can cause severe muscle wasting, which can be inhibited by the activation of PI3K–Akt–FoxO signaling (Wang et al., 2006). We demonstrate here for the first time that plakoglobin is an important constituent of skeletal muscle where it binds to both the insulin receptor and the p85 regulatory subunit of PI3K to enhance signaling by the PI3K–Akt–FoxO cascade. Surprisingly, changes in plakoglobin levels alone influence PI3K–Akt–FoxO pathway in muscle and thereby can cause muscle growth or block atrophy. Thus, Trim32 functions as a novel inhibitor of PI3K–Akt–FoxO signaling by regulating plakoglobin–PI3K binding, which is important for activation of this pathway in muscle and probably most tissues.

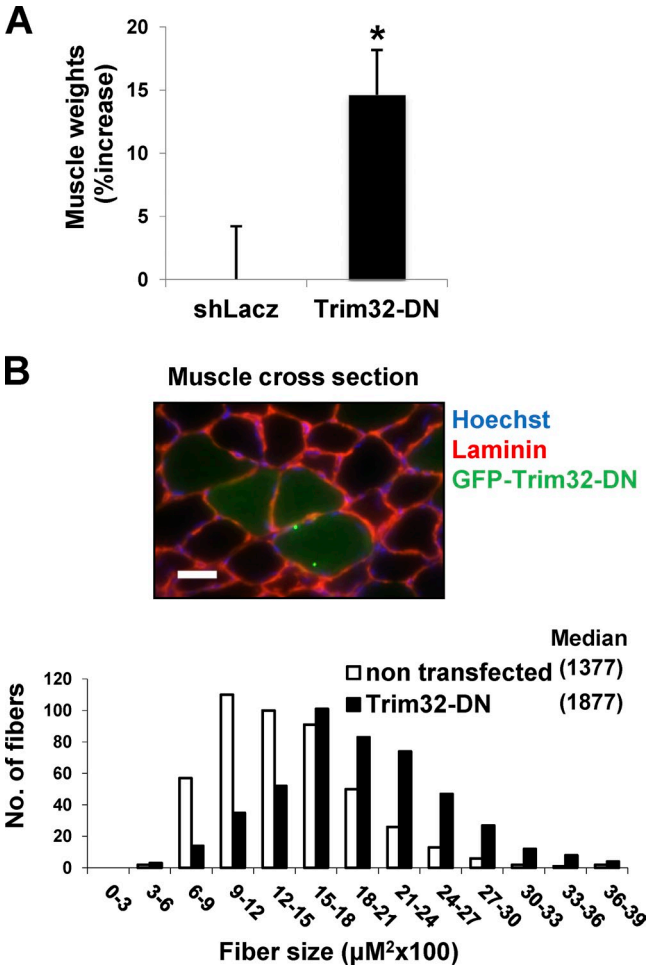

Figure 1. **Inhibition of Trim32 in normal muscle induces rapid growth.** TA muscles were electroporated with shLacz or Trim32-DN and analyzed 6 d later. (A) Mean weights of Trim32-DN–expressing muscles are presented as percent increase versus control. $n = 10$; *, $P < 0.05$. (B) Cross-sectional areas of 500 fibers transfected with GFP-Trim32-DN (black vs. 500 nontransfected fibers [open] in the same muscle. $n = 6$. Laminin staining is in red. Bar, 15 µm.

Results

Trim32 inhibition induces normal muscle growth

Because down-regulation of Trim32 reduces muscle atrophy (Cohen et al., 2012), we determined whether it also affects the mass of normal muscles by electroporation into tibialis anterior (TA) muscle of a dominant-negative Trim32 (Trim32-DN), which lacks the catalytic RING domain and is fused to GFP to identify the transfected fibers (Kano et al., 2008). Overexpression of Trim32-DN for 6 d resulted in a 15% increase in weight over that of muscles electroporated with a control vector (Fig. 1 A). Because not all fibers were transfected, the growth induced by Trim32 inhibition must be even greater. In fact, the mean cross-sectional area of 500 fibers expressing Trim32-DN was much larger than that of 500 nontransfected ones (Fig. 1 B). The Trim32-DN inhibits the endogenous Trim32, although some of the overexpressed Trim32 seemed to form intracellular aggregates (Locke et al., 2009; Ichimura et al., 2013), as often occurs upon overexpression of proteins containing coiled-coil domains that mediate protein interactions and multimerization. Thus, Trim32 seems to function in normal postnatal muscle to limit fiber growth, and suppression of its activity alone can induce muscle hypertrophy.

Plakoglobin is present in skeletal muscle

These findings and our prior ones (Cohen et al., 2012) imply that certain Trim32 substrates accumulate upon its down-regulation and reduce atrophy or induce growth. Using immobilized GST-Trim32 and mass spectrometry (Cohen et al., 2012), we identified several Trim32 substrates in muscle extracts (Cohen et al., 2012) that were bound and could be ubiquitinated by Trim32, including thin-filament and Z-band components, plus the cytoskeletal protein desmin. Surprisingly, the immobilized Trim32 also bound plakoglobin, which, in other tissues, is a component of the desmosome complex. Its presence was unexpected because there had been no prior reports of desmosomes or its components in skeletal muscle. During fasting, however, Trim32

does not significantly reduce plakoglobin content (Fig. S1) or stability (see Fig. 3 A), but clearly alters its function, as discussed in Fig. 3.

In epithelial cells, binding of PI3K to plakoglobin was proposed to enhance PI3K–Akt signaling (Woodfield et al., 2001; Calautti et al., 2005). Because this pathway is the primary regulator of the mass of muscle and probably all eukaryotic cells, we investigated whether its activity is affected by the levels of plakoglobin and Trim32. However, it was important initially to confirm that plakoglobin is actually present in the muscle fibers and not endothelial cells. Therefore, we analyzed its spatial distribution in normal TA by immunofluorescence staining of paraffin-embedded cross and longitudinal sections. In epithelia, plakoglobin has a punctate distribution throughout the cell (Näthke et al., 1994; Chen et al., 2002). We found a similar spot-like distribution of plakoglobin within the muscle fibers, and in the plane of the fiber membrane (Fig. 2 A). Thus, this protein, unlike myofibrillar components or desmin (Cohen et al., 2012), did not show a specific periodic distribution along the sarcomere. A similar diffuse distribution of plakoglobin was observed in C2C12 myotubes (Fig. 2 A).

Furthermore, the presence of this protein in both the soluble phase and the muscle membrane was confirmed biochemically by fractionation of TA muscle (Fig. 2 B). To further support these findings, we performed immunofluorescence staining of muscle cross sections with plakoglobin and dystrophin antibodies. As shown in Fig. 2 C, plakoglobin colocalized with the membrane protein dystrophin (Fig. 2 C). Interestingly, plakoglobin also co-localized with the muscle stem cell marker, the transcription factor Pax 7, indicating that plakoglobin is also present in satellite cells (Fig. 2 D). The finding of plakoglobin in satellite cells is consistent with its presence in cultured myoblasts (see Fig. 4 D) and with its playing an important role in the development of striated muscle (Ruiz et al., 1996; Asimaki et al., 2007).

Trim32 knockdown in fasting increases PI3K–Akt–FoxO signaling

Because plakoglobin in muscle extracts was bound to Trim32, we determined whether it is lost during fasting and the role of Trim32 in this process. Interestingly, whether or not Trim32 was down-regulated by electroporation, the muscle content of plakoglobin did not change during fasting from that in the fed control (which expressed a control shRNA; Fig. 3 A). Thus, during fasting, plakoglobin is not directed for degradation by Trim32, and the interaction between Trim32 and plakoglobin is probably mediated by additional associated proteins.

To determine whether plakoglobin influences the activity of the PI3K–Akt–FoxO pathway, as had been suggested in keratinocytes (Calautti et al., 2005), we investigated whether plakoglobin interacts with p85–PI3K in muscle. Plakoglobin could be coprecipitated with p85–PI3K from muscles of the fed mice, but not during fasting (Fig. 3 A), where PI3K–Akt–FoxO signaling was reduced (Fig. 3 C). This change in plakoglobin association seemed to result from Trim32 function because inhibition of Trim32 during fasting by electroporation of Trim32-DN resulted in a greater association of plakoglobin with p85–PI3K (Fig. 3 A). Thus, during fasting, Trim32 reduces the association of plakoglobin with p85–PI3K. In addition, we determined if these interactions were unique to skeletal muscle or whether plakoglobin might regulate this signaling pathway generally. Similar interactions between p85–PI3K and plakoglobin were demonstrated by coimmunoprecipitation in the heart and liver (Fig. 3 B), and thus are probably functioning in most, perhaps all, cells.

Further studies determined whether the interaction of plakoglobin with p85–PI3K in fact influences PI3K–Akt–FoxO signaling. By two days after food deprivation, phosphorylation of PI3K, Akt, and its target FoxO3, as well as the mTOR target S6K was markedly reduced (Fig. 3 C; Sandri et al., 2004; Stitt et al., 2004). However, down-regulation of Trim32 almost completely blocked this response to fasting. In fact, the levels of phosphorylated PI3K, Akt, FoxO3, and S6K were similar to those in muscles from fed mice (Fig. 3 C). Normally during fasting, FoxO is activated (dephosphorylated) and stimulates the expression of a set of atrophy-related genes, including the ubiquitin ligases MuRF1 and Atrogin1, which are essential for rapid fiber atrophy (Fig. 3 D; Bodine et al., 2001; Gomes et al., 2001). However, Trim32 inhibition by overexpression of the Trim32-DN resulted in a marked decrease in MuRF1 and Atrogin1 expression in the TA muscles during fasting (Fig. 3 D). This inhibition of atrogene expression during fasting together with the maintenance of normal PI3K–Akt–mTOR signaling can account for the dramatic blockage of muscle wasting observed previously (Cohen et al., 2012). Thus, during fasting, Trim32 function is critical in causing the reduction in PI3K–Akt–FoxO signaling that triggers the decrease in protein synthesis, the FoxO-mediated expression of the atrogene program, and muscle wasting (Cohen et al., 2012).

Plakoglobin mediates the effects of Trim32 on PI3K–Akt signaling

To learn whether plakoglobin influences PI3K–Akt–FoxO signaling, we down-regulated plakoglobin by electroporation of shRNA (shJUP) into normal muscle (Fig. 4 A). The resulting fall in plakoglobin led to decreased phosphorylation of PI3K, Akt, and FoxO3. Thus, plakoglobin is required for normal signaling through the PI3K–Akt–FoxO pathway. Accordingly, when plakoglobin was down-regulated with shRNA in normal muscle for 6 d, atrophy of the muscle fibers became evident (Fig. 4 B). The mean cross-sectional area of 500 fibers expressing shJUP (and GFP to identify transfected fibers) was smaller than that of 500 nontransfected fibers (Fig. 4 B). Although expressing the Trim32-DN prevented the decrease in PI3K–Akt–FoxO signaling in the atrophying muscles, this effect was markedly attenuated by simultaneously down-regulating plakoglobin (Fig. 4 C). Thus, plakoglobin appears critical for the Trim32-induced reduction in phosphorylation of PI3K, Akt, and FOXO3 (Fig. 4 C).

In addition to regulating cell size and protein balance, the PI3K–Akt–FoxO pathway also mediates insulin's stimulation of glucose uptake into muscle and adipose tissue. As predicted, plakoglobin down-regulation in myoblasts reduced the stimulation by insulin of glucose uptake (Fig. 4 D). Although plakoglobin is clearly an important regulator of this process, overexpression of

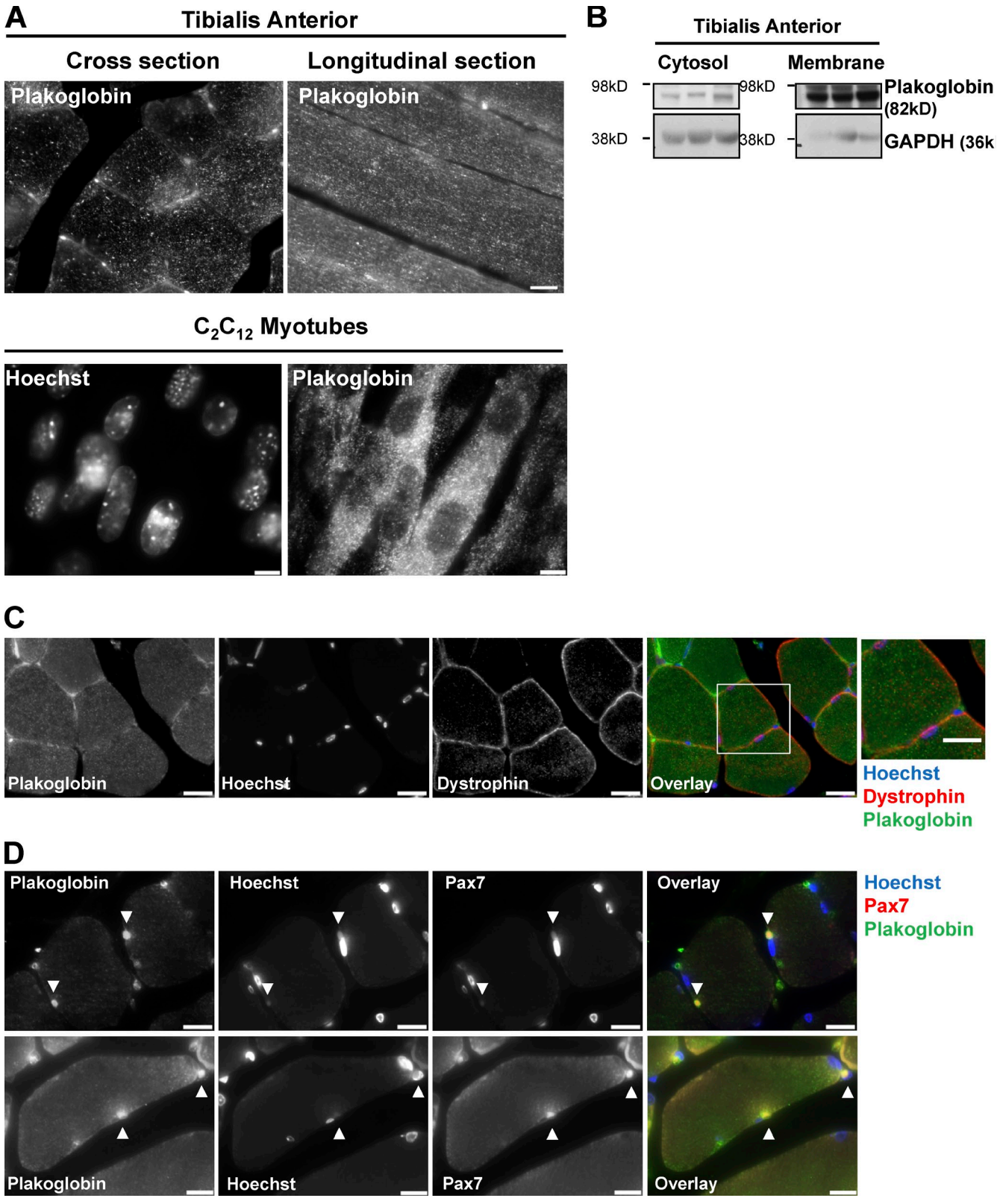

Figure 2. **Plakoglobin is present in skeletal muscle.** (A) Paraffin-embedded longitudinal and cross sections of TA muscles from fed mice (top; bar, 20 µm), and C2C12 myotubes (bottom; bar, 15 µm) were stained with anti-plakoglobin. (B) Plakoglobin is present in the cytosolic and membrane fractions of muscle. 0.25% of membrane fraction and 0.01% of cytosolic fraction were analyzed by immunoblotting. GAPDH serves as a cytosolic marker. (C) Plakoglobin is present on the muscle membrane. Paraffin-embedded cross sections of normal TA muscles were stained with anti-plakoglobin and anti-dystrophin. Bar, 20 µm. The box on the right indicates an area of magnification (bar, 4.3 µm). (D) Plakoglobin is present in satellite cells. Paraffin–embedded cross sections of normal TA muscles were stained with anti-plakoglobin and anti-pax7 antibodies. Bar, 12 µm.

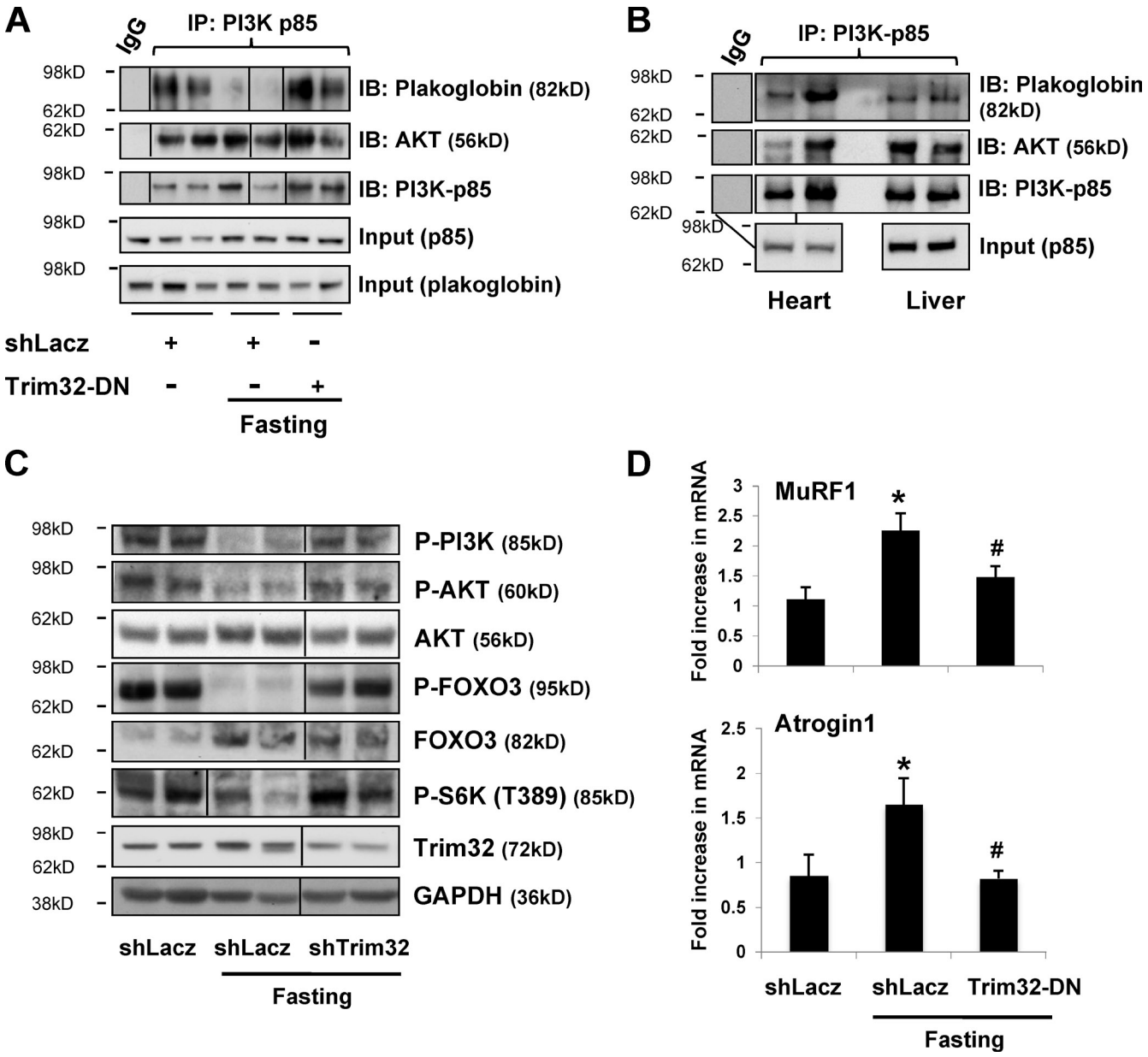

Figure 3. **Trim32 down-regulation during fasting enhances plakoglobin binding to PI3K–p85 and PI3K–Akt–FoxO signaling.** (A) During fasting, inhibition of Trim32 increases the interaction of plakoglobin with p85–PI3K. p85–PI3K was immunoprecipitated from the soluble fraction of muscles expressing shLacz or Trim32-DN from fed or fasted mice. Precipitates were analyzed by immunoblotting. Black lines indicate the removal of intervening lanes for presentation purposes. (B) Plakoglobin and p85–PI3K interact in heart and liver. p85–PI3K was immunoprecipitated from the soluble fraction of heart and liver from fed mice and analyzed by immunoblotting. The lines connecting the two bottom panels show the input lane for the heart sample that was used for two immunoprecipitation reactions using IgG (for control) or PI3K antibody. (C) During fasting, down-regulation of Trim32 increases PI3K–Akt–FoxO signaling. Soluble fractions of normal and atrophying muscles expressing shLacz or shTrim32 were analyzed by SDS-PAGE and immunoblot. Black lines indicate the removal of intervening lanes for presentation purposes. (D) Inhibition of Trim32 reduces MuRF1 and Atrogin1 expression during fasting. Quantitative RT-PCR of mRNA preparations from atrophying and control muscles expressing shLacz or Trim32-DN using primers for MuRF1 and Atrogin1. Data are plotted as the mean fold change relative to fed control. $n = 4$. *, $P < 0.05$ vs. shLacz in fed. #, $P < 0.05$ vs. shLacz in fasting.

plakoglobin in normal myoblasts did not further stimulate this process (Fig. 4 D). Cytochalasin B is a cell-permeable mycotoxin that competitively inhibits glucose transport into cells and was used here to evaluate specifically regulated glucose uptake (Ebstensen and Plagemann, 1972). To test if plakoglobin mediates insulin-dependent glucose uptake by interacting with the insulin receptor and activating PI3K–Akt–FoxO signaling, we immunoprecipitated plakoglobin from normal and atrophying muscles. The insulin receptor coprecipitated together with plakoglobin from normal muscle. Interestingly, during fasting, plakoglobin remained associated with the insulin receptor (Fig. 4 E), even when Trim32 was inhibited by electroporation of Trim32-DN (Fig. 4 E). Plakoglobin thus binds to the insulin receptor and seems to serve as a key component in its interactions with and activation of PI3K. This interaction has been confirmed in a reciprocal experiment with both normal and atrophying muscles where immunoprecipitation of the insulin receptor also brought down plakoglobin (Fig. 4 E). Similar

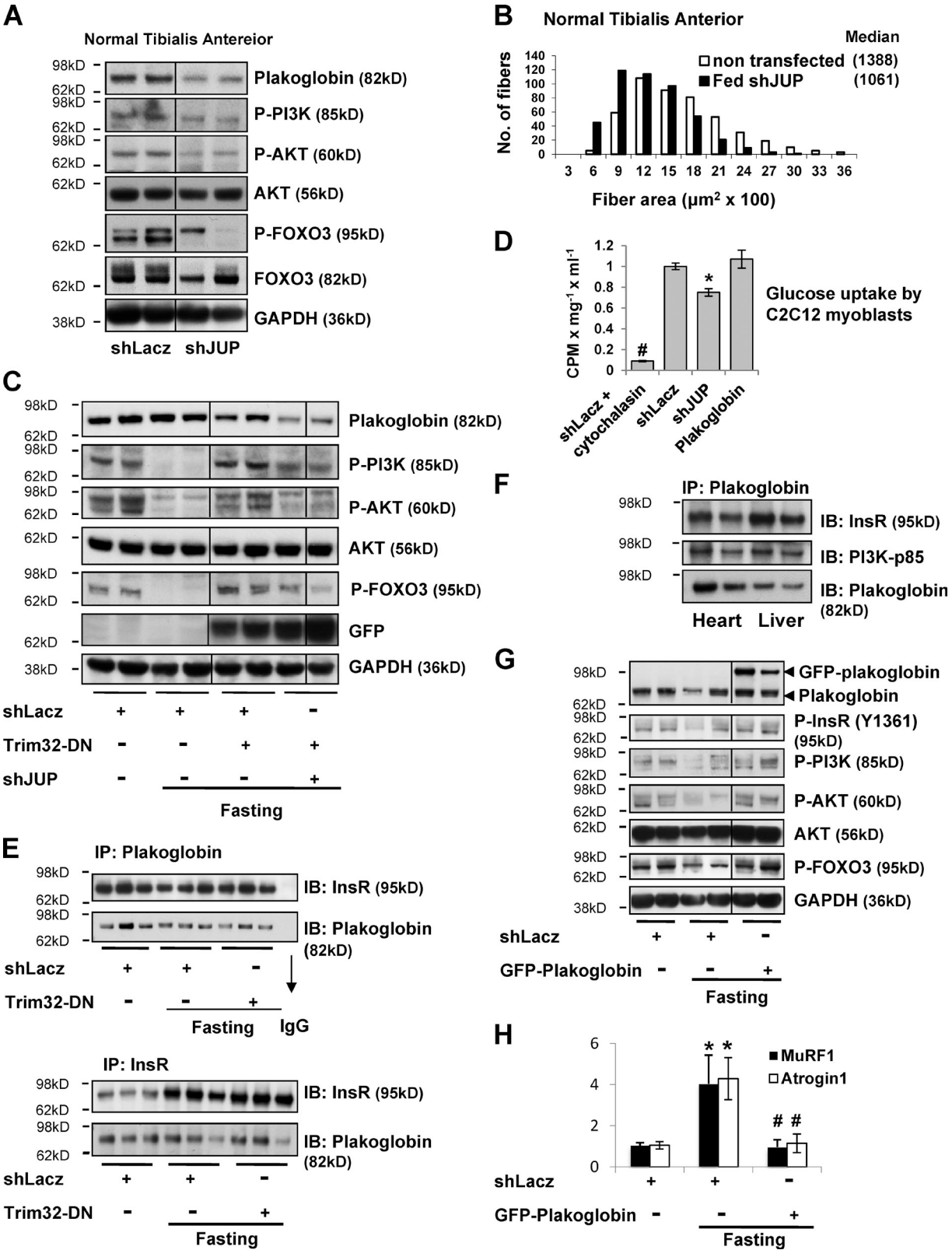

Figure 4. **Plakoglobin down-regulation reduces PI3K–Akt–FoxO signaling, glucose uptake, and fiber size.** (A) Plakoglobin knockdown with shJUP results in reduced PI3K–Akt–FoxO signaling. Normal TA muscles were transfected with shLacz or plakoglobin shRNA (shJUP), and soluble extracts were analyzed by SDS-PAGE and immunoblot. Black lines indicate the removal of intervening lanes for presentation purposes. (B) Down-regulation of plakoglobin induces muscle atrophy. Cross-sectional areas of 500 fibers transfected with shJUP (that express GFP, black bars) vs. 500 nontransfected fibers (open bars) in the same muscle. $n = 6$. (C) During fasting, down-regulation of plakoglobin reduces the increase in PI3K–Akt–FoxO signaling induced by Trim32-DN. Soluble fractions of muscles expressing shLacz alone, Trim32-DN together with shLacz, or Trim32-DN together with shJUP were analyzed by SDS-PAGE and immunoblot. Black lines indicate the removal of intervening lanes for presentation purposes. (D) Plakoglobin down-regulation in C2C12 myoblasts

interactions between plakoglobin and the insulin receptor were also observed in heart and liver (Fig. 4 F), suggesting that, in many tissues (perhaps all), plakoglobin functions to regulate insulin-dependent activation of PI3K.

Together, these observations suggested that increasing the level of plakoglobin during fasting should lead to greater activity of the insulin receptor and PI3K–Akt–FoxO pathway. Accordingly, during fasting, overexpression of GFP-tagged plakoglobin (which showed a similar distribution as did the endogenous protein; Fig. S2) alone enhanced phosphorylation of the insulin receptor (at Y1361), activation of PI3K–Akt–FoxO signaling (Fig. 4 G), and reduced MuRF1 and Atrogin1 expression (Fig. 4 H). Thus, the Trim32-dependent inhibition of plakoglobin function is a key new step in the reduction in PI3K–Akt–FoxO signaling in low-insulin states.

Trim32 inhibition enhances PI3K–Akt–FoxO signaling in normal muscle

In light of these findings during fasting, we determined whether Trim32 may also influence muscle mass (Fig. 1) in the fed state by regulating PI3K–Akt–FoxO activity. After electroporation of the Trim32-DN or shTrim32 into normal TA for 6 d, phosphorylation of PI3K, Akt, and FOXO increased (Fig. 5 A). The levels of mTOR targets pS6K and p704E-BP1 were also increased (Fig. 5 A), indicating stimulation of mTOR by the inhibition of Trim32. Accordingly, transfection of Trim32-DN into C2C12 myoblasts enhanced insulin-dependent glucose uptake above the levels in cells expressing a control plasmid (Fig. 5 B), and inhibition of Trim32 in normal muscle increased the association of plakoglobin with PI3K–p85 (Fig. 5 C). Thus, the growth-promoting effects of Trim32-DN are most probably due to enhanced PI3K–Akt–mTOR signaling. It is noteworthy that Trim32 overexpression in normal muscle does not by itself alter PI3K–Akt–FoxO signaling, glucose uptake, or fiber size (Fig. 5 B; Fig. S3). Therefore, an additional signal beyond Trim32 expression is probably required to decrease plakoglobin function, perhaps phosphorylation of plakoglobin (Woodfield et al., 2001; Calautti et al., 2005).

Discussion

These studies have uncovered a novel mechanism regulating the PI3K–Akt–FoxO pathway that involves the desmosomal component plakoglobin and the ubiquitin ligase, Trim32 (Fig. 6). Because decreasing plakoglobin content reduces glucose uptake (Fig. 4 D), whereas increasing plakoglobin levels stimulates this process (Figs. 4 G and 5 B), Trim32-mediated inhibition of plakoglobin function may also contribute to insulin resistance in various catabolic states (e.g., diabetes, metabolic syndrome, or sepsis). Consequently, Trim32 may represent a new therapeutic target to block muscle wasting and the insulin resistance characteristic of many disease states (e.g., cancer cachexia, sepsis, and renal failure).

In normal muscle, plakoglobin down-regulation reduces PI3K–Akt–FoxO signaling and causes atrophy (Fig. 4, A and B), whereas inhibiting Trim32 increases plakoglobin binding to PI3K–p85, enhances PI3K–Akt–FoxO phosphorylation, and induces fiber hypertrophy (Figs.1 and 5). Thus, in addition to being critical in atrophy, Trim32 activity also limits the growth of normal muscle (Fig. 6). Moreover, Trim32 and plakoglobin probably serve similar regulatory roles in controlling the growth of other cells because both are expressed in most, if not all, tissues (Cowin et al., 1986; Frosk et al., 2002). In fact, plakoglobin has been shown to be an important regulator of epithelial growth (Venkiteswaran et al., 2002), and as shown here, it binds p85–PI3K in heart and liver (Figs. 3 B and 4 F), as it does in skeletal muscle (Figs. 3 A and 5 C). Interestingly, the close homologue of plakoglobin, β-catenin, can also bind PI3K and enhance PI3K–Akt–FoxO signaling (Woodfield et al., 2001). Moreover, β-catenin was reported to decrease during atrophy induced by dexamethasone and to accumulate during hypertrophy (Schakman et al., 2008). Plakoglobin and β-catenin can function together in regulating gene transcription (Zhurinsky et al., 2000a,b; Winn et al., 2002; Armstrong et al., 2006; Li et al., 2011), and possibly β-catenin may also be regulated by Trim32.

Because Trim32 is not induced during fasting, its activity may be regulated by post-translational modifications of its substrates, as we previously demonstrated for desmin (Cohen et al., 2012), or by modifications of Trim32 itself, as has been shown to occur in other tissues (Dephoure et al., 2008; Ichimura et al., 2013). Here we show that Trim32 activity promotes the dissociation of the plakoglobin–PI3K complex and thereby inhibits PI3K–Akt signaling. Even though Trim32, when purified, can weakly ubiquitinate plakoglobin (unpublished data), and though it seems to affect plakoglobin stability in normal muscle (Fig. 5 A), plakoglobin content does not fall in fasting (Fig. 3 A). Thus, in the atrophying muscles, Trim32 does not promote plakoglobin–PI3K dissociation by enhancing plakoglobin degradation. Perhaps Trim32 promotes proteasomal degradation of an additional protein that is essential for the plakoglobin–PI3K complex, and that, like desmin, may be phosphorylated during

reduces insulin-induced glucose uptake. [^{3}H]2-deoxy-D-glucose uptake (cpm) was measured in C2C12 myoblasts expressing shLacz, shJUP, or plakoglobin. Cytochalasin B is a competitive inhibitor of regulated glucose transport into cells. To determine the insulin-dependent glucose uptake, the values measured in the presence of 20 µM cytochalasin B were subtracted from the total uptake. $n = 3$, *, $P < 0.05$ vs. shLacz; #, $P < 0.005$ vs. shLacz. (E) Plakoglobin associates with the insulin receptor in normal and atrophying muscles. Plakoglobin (top) or insulin receptor (bottom) were immunoprecipitated from the soluble fraction of muscles expressing shLacz or Trim32-DN from fed or fasted mice. Precipitates were then analyzed by immunoblotting for insulin receptor and plakoglobin, as indicated. (F) Plakoglobin associates with insulin receptor in heart and liver. Plakoglobin was immunoprecipitated from the soluble fraction of heart and liver from fed mice and analyzed by immunoblotting. (G) During fasting, overexpression of plakoglobin alone activates insulin receptor and enhances PI3K–Akt–FoxO signaling. Soluble fractions of normal and atrophying muscles expressing shLacz or GFP-plakoglobin were analyzed by SDS-PAGE and immunoblot. Black lines indicate the removal of intervening lanes for presentation purposes. (H) Overexpression of plakoglobin reduces MuRF1 and Atrogin1 expression during fasting. Quantitative RT-PCR of mRNA preparations from atrophying and control muscles expressing shLacz or GFP-plakoglobin using primers for MuRF1 and Atrogin1 (and GAPDH for reference). Data are plotted as the mean fold change relative to fed control. $n = 4$. *, $P < 0.05$ vs. shLacz in fed. #, $P < 0.05$ vs. shLacz in fasting.

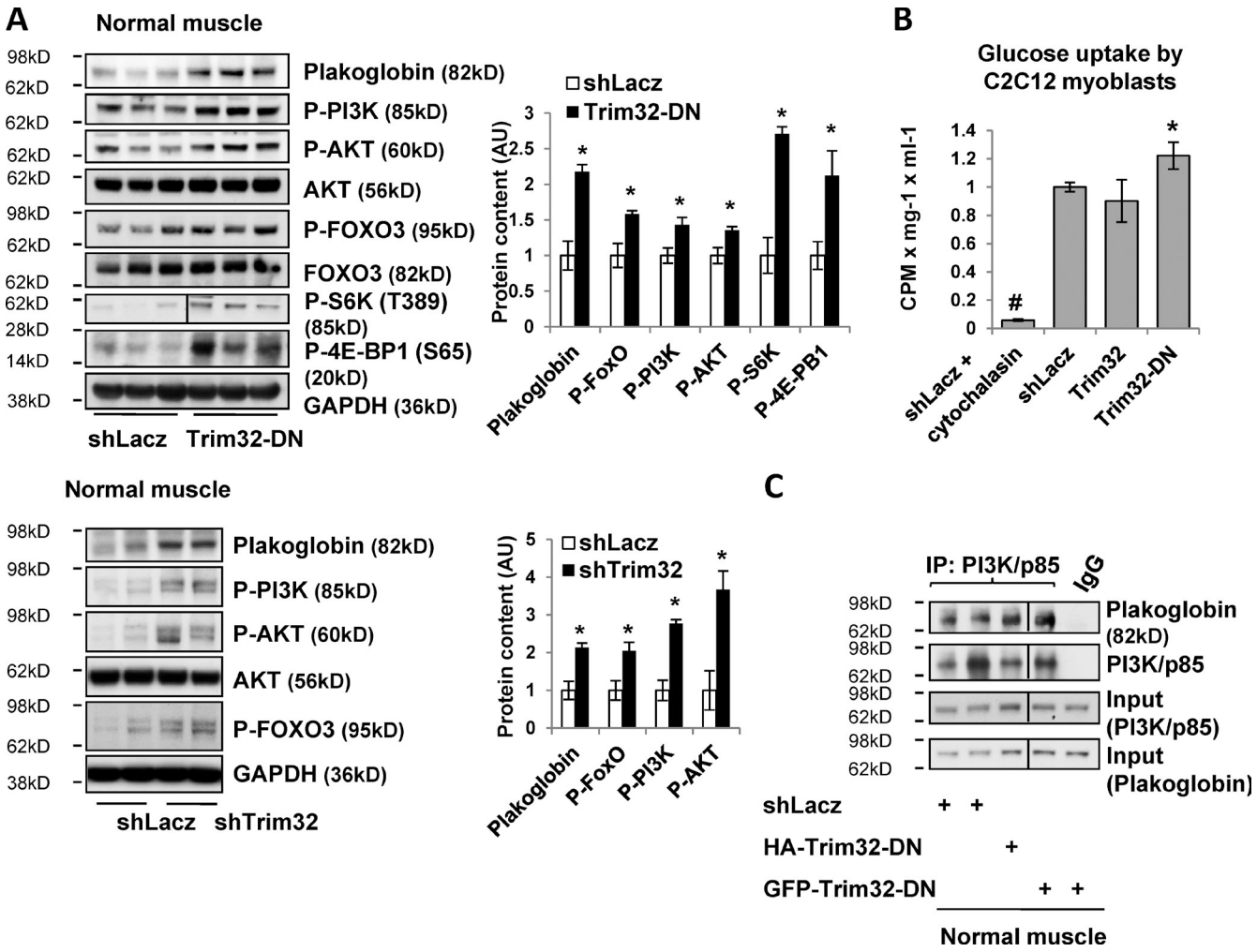

Figure 5. **Trim32 inhibition in normal muscle increases PI3K–Akt–FoxO activity and glucose uptake.** (A) Down-regulation of Trim32 increases PI3K–Akt–FoxO and mTOR activity. (Left) Soluble fractions of normal TA muscles expressing shLacz, Trim32-DN (top), or shTrim32 (bottom) were analyzed by SDS-PAGE and immunoblot. The black line in the P-S6K panel indicates the removal of intervening lanes for presentation purposes. (Right) Densitometric measurement of band intensity in the presented blots. $n = 3$. (B) Trim32 inhibition in C2C12 myoblasts increases insulin-induced glucose uptake. [^{3}H]2-deoxy-D-glucose uptake was measured in C2C12 myoblasts expressing shLacz, Trim32, or Trim32-DN, as in Fig. 4 D. Cytochalasin B is a competitive inhibitor of regulated glucose transport into cells. $n = 3$; *, $P < 0.005$ vs. shLacz; #, $P < 0.005$ vs. shLacz. (C) Inhibition of Trim32 in normal muscle enhances the interaction of plakoglobin with p85–PI3K. p85–PI3K was immunoprecipitated from the soluble fraction of normal muscles expressing shLacz or Trim32-DN. Precipitates were analyzed by immunoblotting. Black lines indicate the removal of intervening lanes for presentation purposes.

atrophy (Cohen et al., 2012), so as to enhance its ubiquitination by Trim32. Alternatively, during fasting, ubiquitination of plakoglobin may occur but lead to p97-mediated dissociation of the plakoglobin–PI3K complex (Piccirillo and Goldberg, 2012). Clearly, the exact mode of regulation of Trim32 activity and the mechanism by which it catalyzes plakoglobin–PI3K dissociation are very important questions for future research.

It is noteworthy, however, that Trim32 overexpression by itself is not sufficient to reduce PI3K–Akt–FoxO activity or to cause atrophy (Fig. S3). Thus, the increase in PI3K–Akt–FoxO signaling with Trim32 down-regulation must involve an additional signal, such as plakoglobin phosphorylation, which has been reported (Woodfield et al., 2001; Calautti et al., 2005). Accordingly, we recently showed that ubiquitination of desmin by Trim32 during fasting also requires desmin phosphorylation (Cohen et al., 2012). In normal muscle and during fasting, if Trim32 is inhibited, phosphorylation of plakoglobin may be essential for its association with the insulin receptor and perhaps for it to serve as a docking site for PI3K. In any case, this selective accumulation of plakoglobin led to increased phosphorylation of the insulin receptor and activity of the PI3K–Akt–FoxO pathway (Fig. 4 G).

To our knowledge, this study also provides the first evidence for the presence of the desmosomal component plakoglobin in skeletal muscle. In these and related studies, we also found that other components of the desmosomal complex, such as desmoplakin, are also present within muscle fibers (Fig. S4), although desmoplakin levels, unlike plakoglobin's, did not alter PI3K–Akt–FoxO signaling (Fig. S4 A). In the heart, plakoglobin is a component of the adhesion complex, i.e., "desmosomes," which are localized in the intercalated discs that link adjacent cardiomyocytes. Mice lacking plakoglobin tend to die early from cardiac rupture (Ruiz et al., 1996), and in humans, mutations in plakoglobin (Asimaki et al., 2007) or the six other

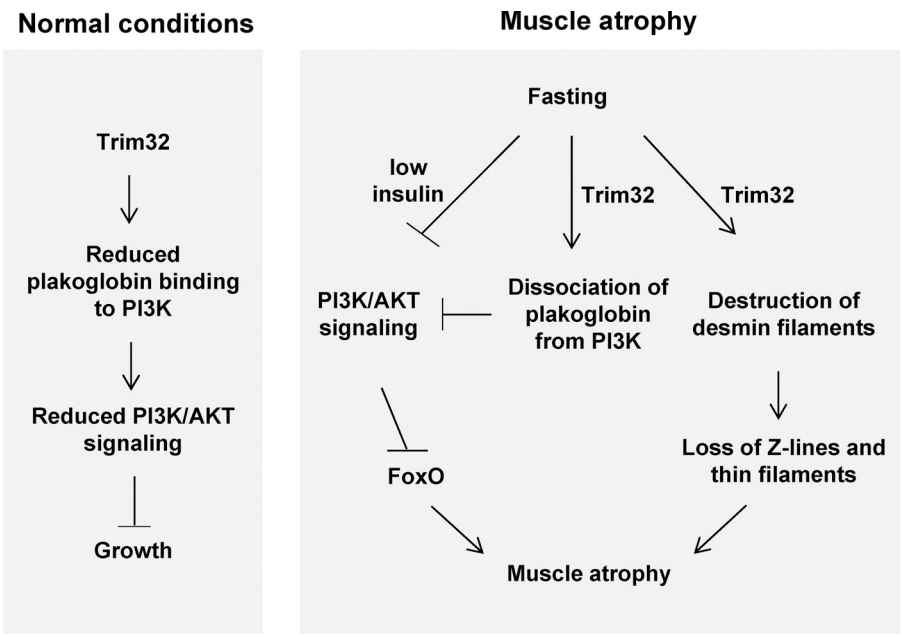

Figure 6. **Proposed new mechanism for regulation of PI3K–Akt–FoxO pathway by Trim32.** By promoting plakoglobin dissociation from PI3K–p85, Trim32 reduces PI3K–Akt–FoxO signaling in normal and atrophying muscle and regulates growth. In addition to its role in myofibril breakdown during fasting (Cohen et al., 2012), Trim32 also functions as a novel inhibitor of PI3K–Akt–FoxO signaling. Because Trim32 and plakoglobin are expressed in most tissues (Cowin et al., 1986; Frosk et al., 2002), they probably serve similar roles in regulating the growth of other cells. This novel mechanism probably contributes to the insulin resistance during fasting and catabolic diseases (e.g., diabetes, sepsis), and perhaps to the myopathies and cardiomyopathies seen with Trim32 and plakoglobin mutations.

genes encoding desmosomal proteins (Herren et al., 2009) result in cardiac arrhythmia (Asimaki et al., 2007), reduced contractility, and cardiac failure (i.e., the syndrome of "arrhythmogenic right ventricular cardiomyopathy/dysplasia"). Perhaps these pathological sequelae may be due in part to altered signaling through the PI3K–Akt–FoxO pathway. By reducing the function of plakoglobin or perhaps other desmosomal components in the heart, Trim32 is also likely to have important physiological or pathological effects. However, in skeletal muscle, plakoglobin does not seem to form the "classic" desmosomes, although this protein is clearly present on the surface membrane (Fig. 2) and can be immunoprecipitated together with insulin receptor, PI3K, and Akt (Figs. 3 A and 4 E), as well as other components of desmosomes (Fig. S4 B). However, unlike dystrophin, plakoglobin does not seem to be evenly distributed along the muscle membrane, and instead accumulates in certain regions, presumably by binding to specific receptors to stimulate signaling pathways or to promote cell–cell contacts. In addition to causing limb-girdle muscular dystrophy, Trim32 mutations can lead to Bardet-Biedl syndrome, which is characterized by cardiac hypertrophy and dilated cardiomyopathy (Elbedour et al., 1994). The present findings would predict that a deficiency of Trim32 could lead to excessive tissue growth and possibly inappropriate activation of PI3K–Akt–FoxO signaling.

Surprisingly, Spencer and colleagues recently described a Trim32-null mouse that exhibited multiple defects, including mild myopathies, neurogenic defects, cellular disorganization, and reduced muscle growth and body size (Kudryashova et al., 2011, 2012). Nevertheless, upon fasting or disuse (Kudryashova et al., 2012), muscles from these mice atrophy to a similar extent, as in wild-type mice. These surprising observations differ markedly from the present findings on the effects of selective down-regulation of Trim32 in adult muscle or myotubes. Presumably, the complete deficiency of Trim32 in all cells during development causes multiple systemic defects and elicits multiple compensatory responses. The ability of these Trim32-deficient muscles to undergo atrophy suggests that additional ubiquitin ligases may replace Trim32 in its many regulatory roles. (In fact, our prior observations had suggested that alternative ligases may also function in atrophy (Cohen et al., 2012)).

Conversely, expression of Trim32 rises in multiple diseases, including the brains of Alzheimer's patients (Yokota et al., 2006), psoriasis lesions (Liu et al., 2010), and various cancers, where it enhances invasion and metastasis (Horn et al., 2004; Kano et al., 2008). These effects may also involve Trim32-mediated regulation of plakoglobin stability or function because the loss of plakoglobin reduces cell adhesion and increases cell migration and invasion (Yin et al., 2005; Kundu et al., 2008; Gosavi et al., 2011).

Together, these observations indicate close coupling between changes in cytoskeletal and myofibrillar components during atrophy (Cohen et al., 2012) and the cell's major growth regulatory system. This coupling could be important in other pathological states (Fig. 6). During atrophy, Trim32 catalyzes the ubiquitination and disassembly of the desmin cytoskeleton, which is coupled to the destruction of proteins comprising the thin filament and Z-band (Cohen et al., 2012). If desmin filaments in skeletal muscle are also linked to plakoglobin (and other desmosomal proteins), as they are in the heart (Smith and Fuchs, 1998), then perturbation of plakoglobin function during atrophy, in addition to reducing PI3K–Akt–FoxO signaling, may be an early event leading to the disruption of the cytoskeleton and thereby to disassembly of thin filaments.

Materials and methods

In vivo transfection

Animal experiments were conducted according to the ethical guidelines of the National Institutes of Health Guide for the Care and Use of Laboratory Animals. Animal care was provided by specialized personnel in the Institutional Animal Care facility. Experiments were performed in adult CD-1 male mice (27–28 g). In vivo electroporation was performed by the injection

of 20 µg of plasmid DNA into adult mouse TA muscle and application of mild electric pulses (12V, 5 pulses, 200-ms intervals; Cohen et al., 2012). In fasting experiments food was removed from cages 4 d after electroporation for 48 h. Fiber size was determined by measurements of cross-sectional area of 500 transfected (express GFP) and 500 adjacent nontransfected fibers in the same muscle section (10 µm), using MetaMorph software (Molecular Devices).

Antibodies and constructs

The Trim32 and control shRNAs (Cohen et al., 2012), as well as the plakoglobin and desmoplakin shRNA, were designed using Invitrogen's BLOCK-iT RNAi expression vector kit with the pcDNA 6.2-GW/EmGFP-miR vector. The GFP-plakoglobin vector was provided by M. Dunach (Autonomous University of Barcelona, Barcelona, Spain). The Trim32-DN and Trim32 plasmids (both also encode GFP, which allows identification of the transfected fibers) were provided by M. Kules-Martin (Oregon Health and Science University, Portland, OR), and the HA-Trim32 construct by S. Hatakeyama (Hokkaido University Graduate School of Medicine, Sapporo, Japan). Plakoglobin antibodies were from GeneTex and Sigma-Aldrich. Anti-laminin and GAPDH were from Sigma-Aldrich. Anti-tubulin was from Invitrogen, and anti-GFP and anti-dystrophin from Abcam. The Pax7 antibody was developed by A. Kawakami (Tokyo Institute of Technology, Yokohama, Japan) and obtained from the Developmental Studies Hybridoma Bank developed under the auspices of the NICHD and maintained by The University of Iowa, Department of Biology (Iowa City, IA). Anti-HA, Akt, P-Akt, PI3K–p85, P-PI3K–p85, FOXO3, P-FOXO3, insulin receptor, P-insulin receptor (Y1361), p70S6K, and p4E-BP1 were from Cell Signaling Technology. The desmoplakin antibody was purchased from Santa Cruz Biotechnology, Inc., and the Trim32 antibody was provided by J. Schwamborn (ZMBE Institute of Cell Biology, Münster, Germany).

Fractionation of muscle tissue

Work was performed at 4°C. Mouse TA muscles were homogenized on ice for 30 s in 19 vol of buffer C (20 mM Tris-HCl, pH 7.6, 5 mM EDTA/NaOH, pH 7.4, 100 mM KCl, 1 mM DTT, and 1 mM sodium orthovanadate) and spun at 2,900 *g* for 20 min to pellet nuclei and unbroken tissue. The supernatant was centrifuged at 180,000 *g* for 90 min and the supernatant (i.e., cytosolic fraction) stored at −80°C. The pellet was resuspended in 10 vol of buffer M (20 mM Tris-HCl, pH 7.6, 5 mM EDTA/NaOH, pH 7.4, 100 mM KCl, 1 mM DTT, 0.25% sodium deoxycholate, 1% NP-40, and 1 mM sodium orthovanadate), rotated at 4°C for 20 min, and centrifuged at 100,000 *g* for 30 min. The supernatant (i.e., membrane fraction) was then collected and stored at −80°C. All buffers contained protease inhibitors (10 µg/ml leupeptin, 3 mM benzamidine, 1 µg/ml trypsin inhibitor, and 1 mM PMSF). 0.25% of membrane fraction and 0.01% of cytosolic fraction were separated on SDS-PAGE for Western blot analysis.

For the immunoblotting and immunoprecipitation experiments, muscles were homogenized in cold extraction buffer (20 mM Tris-HCl, pH 7.2, 5 mM EGTA, 100 mM KCl, 1% Triton X-100, 10 µg/ml leupeptin, 10 µg/ml pepstatin, 3 mM benzamidine, 1 µg/ml trypsin inhibitor, and 1 mM PMSF) and incubated at 4°C for 1 h with gentle agitation. After centrifugation at 3,000 *g* for 30 min at 4°C, the supernatant (i.e., cytosolic fraction) was stored at −80°C. Phosphatase inhibitors were not added to extraction buffer except for the immunoprecipitation experiments and blots presented in Fig. 5 (1 mM Na_3VO_4 and 50 mM NaF).

Protein analysis

Immunoblotting and immunoprecipitation were performed as described in Cohen et al. (2009). In brief, the cytosolic fraction from TA muscle was used for immunoblotting or immunoprecipitation and was resolved by SDS-PAGE and immunoblotting with specific antibodies and secondary antibodies conjugated to alkaline phosphatase. Immunoprecipitation assays of plakoglobin or PI3K–p85 from the soluble fraction of muscle were performed overnight at 4°C and then protein A/G agarose was added for 4 h.

Quantitative real-time PCR

Total RNA was isolated from muscle and cDNA synthesized by reverse transcription. Real-time qPCR was performed on mouse target genes using specific primers (Table S1) and DyNAmo HS SYBR Green qPCR kit (F-410S; Finnzymes) according to the manufacturer's protocol.

Immunofluorescence

Immunofluorescence of paraffin-embedded muscle sections was performed as reported previously (Cohen et al., 2012). In brief, muscle cross or longitudinal sections from fed and fasted mice were embedded in paraffin and then gradually rehydrated in ethanol/PBS. For immunofluorescence of rehydrated samples 1:50 dilution of anti-plakoglobin, laminin, or dystrophin; 1:5 dilution of pax7 antibody (supernatant), and 1:1,000 dilution of Alexa Fluor 555– or 647–conjugated secondary antibody were used. Images were collected at room temperature using an upright fluorescent microscope (model 80i; Nikon), with Plan Apochromat 60× (Fig. 2 C) or 100× (Fig. 2 D) objective lenses, a 545/30 excitation filter, and 620/60 emission filter (Alexa Fluor 555); a 620/60 excitation filter and 700/75 emission filter (Alexa Fluor 647); a cooled CCD camera (ORCA-R2; Hamamatsu Photonics), and MetaMorph 7 software. In Fig. S2, a vector encoding GFP-plakoglobin was electroporated into TA of adult wild-type mouse for 6 d. Muscle cross sections were embedded in paraffin and images were collected at room temperature using an upright epifluorescence microscope (model 80i; Nikon) with a Plan Fluor 40× 1.4 NA objective lens, a 480/40 excitation filter and 535/50 emission filter, and a cooled CCD camera (model C8484-03; Hamamatsu Photonics).

In Fig. 2 A, C2C12 cells were plated on a glass-bottom 12-well plate (P12G-1.5-14-F; MatTek Corporation), which was coated with 5 ug/ml fibronectin (f1141; Sigma-Aldrich). Cells were differentiated into myotubes and then fixed in 4% PFA for 15 min at room temperature. After 15 min of blocking in 50 mg/ml BSA/TBS-T, immunofluorescence analysis was performed using a 1:50 dilution of plakoglobin antibody and 1:1,000 dilution of Alexa Fluor 555–conjugated secondary antibody, all diluted in blocking solution. Images were collected at room temperature using an inverted motorized microscope (model Ti-E; Nikon) with a Plan Apochromat 1.4 NA 60× objective lens, a 545/30 excitation filter and 620/60 emission filter (Alexa Fluor 555), a cooled CCD camera (ORCA-R2; Hamamatsu Photonics), and MetaMorph 7 software.

Glucose uptake assay

C2C12 cells were plated on a 6-well plate coated with 5 ug/ml fibronectin (f1141; Sigma-Aldrich). 42 h after transfection (with Lipofectamine 2000), cells were washed in warm PBS, starved in DMEM/0.1% BSA for 6 h, and washed again. After treatment with 200 nM insulin/PBS (I0516; Sigma-Aldrich) for 30 min at 37°C, cells were washed and incubated for 10 min at 37°C with 1 uCi/ml 2-deoxy-D-[^{3}H]glucose (NET328A250UC; PerkinElmer) and 0.1 mM cold 2-deoxy-D-glucose (D8375; Sigma-Aldrich). 20 nM of cytochalasin B (glucose transport inhibitor; C6762; Sigma-Aldrich) was added to control wells. Then, cells were washed in cold PBS, lysed in 0.2 N NaOH for 2 h at room temperature, and radioactivity was determined using scintillation fluid.

Statistical analysis and image acquisition

Data are presented as means ± SEM. The statistical significance was determined with one-tailed paired Student's *t* test. Alpha level was set to 0.05. Muscle sections were imaged at room temperature with an upright fluorescent microscope (model 80i; Nikon) and a monochrome camera (model C8484-03; Hamamatsu Photonics), and C2C12 myotubes with an inverted motorized microscope (model Ti-E; Nikon) and a cooled CCD camera (ORCA-R2; Hamamatsu Photonics). Image acquisition and processing was performed using MetaMorph software. Black and white images were processed with Photoshop CS3 software, version 10.0.1 (Adobe).

Online supplemental material

Fig. S1 shows that plakoglobin expression (mRNA levels) does not change during fasting. Fig. S2 shows the distribution of GFP-plakoglobin in muscle, which is similar to the endogenous protein. Fig. S3 shows that overexpression of Trim32 in normal muscle for 10 d does not induce fiber atrophy and does not reduce signaling through the PI3K–Akt pathway. Fig. S4 shows that the desmosomal component desmoplakin interacts with plakoglobin in skeletal muscle but is not essential for PI3K–Akt–FoxO signaling. Table S1 lists the qPCR primers and shRNA oligos which were used in the present study. Online supplemental material is available at http://www.jcb.org/cgi/content/full/jcb.201304167/DC1. Additional data are available in the JCB DataViewer at http://dx.doi.org/10.1083/jcb.201304167.dv.

We thank the Nikon Imaging Center at Harvard Medical School for their assistance with fluorescence microscopy.

This project was supported by grants from the National Institute of Aging, Muscular Dystrophy Association, and the Packard Foundation to A.L. Goldberg, and a stipend to S. Cohen from the International Sephardic Education Foundation (ISEF).

The authors declare no competing financial interests.

Submitted: 25 April 2013
Accepted: 23 January 2014

References

Armstrong, D.D., V.L. Wong, and K.A. Esser. 2006. Expression of beta-catenin is necessary for physiological growth of adult skeletal muscle. *Am. J. Physiol. Cell Physiol.* 291:C185–C188. http://dx.doi.org/10.1152/ajpcell.00644.2005

Asimaki, A., P. Syrris, T. Wichter, P. Matthias, J.E. Saffitz, and W.J. McKenna. 2007. A novel dominant mutation in plakoglobin causes arrhythmogenic right ventricular cardiomyopathy. *Am. J. Hum. Genet.* 81:964–973. http://dx.doi.org/10.1086/521633

Bodine, S.C., E. Latres, S. Baumhueter, V.K. Lai, L. Nunez, B.A. Clarke, W.T. Poueymirou, F.J. Panaro, E. Na, K. Dharmarajan, et al. 2001. Identification of ubiquitin ligases required for skeletal muscle atrophy. *Science*. 294:1704–1708. http://dx.doi.org/10.1126/science.1065874

Buxton, R.S., P. Cowin, W.W. Franke, D.R. Garrod, K.J. Green, I.A. King, P.J. Koch, A.I. Magee, D.A. Rees, J.R. Stanley, et al. 1993. Nomenclature of the desmosomal cadherins. *J. Cell Biol.* 121:481–483. http://dx.doi.org/10.1083/jcb.121.3.481

Calautti, E., J. Li, S. Saoncella, J.L. Brissette, and P.F. Goetinck. 2005. Phosphoinositide 3-kinase signaling to Akt promotes keratinocyte differentiation versus death. *J. Biol. Chem.* 280:32856–32865. http://dx.doi.org/10.1074/jbc.M506119200

Chen, X., S. Bonne, M. Hatzfeld, F. van Roy, and K.J. Green. 2002. Protein binding and functional characterization of plakophilin 2. Evidence for its diverse roles in desmosomes and beta-catenin signaling. *J. Biol. Chem.* 277:10512–10522. http://dx.doi.org/10.1074/jbc.M108765200

Cohen, S., J.J. Brault, S.P. Gygi, D.J. Glass, D.M. Valenzuela, C. Gartner, E. Latres, and A.L. Goldberg. 2009. During muscle atrophy, thick, but not thin, filament components are degraded by MuRF1-dependent ubiquitylation. *J. Cell Biol.* 185:1083–1095. http://dx.doi.org/10.1083/jcb.200901052

Cohen, S., B. Zhai, S.P. Gygi, and A.L. Goldberg. 2012. Ubiquitylation by Trim32 causes coupled loss of desmin, Z-bands, and thin filaments in muscle atrophy. *J. Cell Biol.* 198:575–589. http://dx.doi.org/10.1083/jcb.201110067

Cowin, P., H.P. Kapprell, W.W. Franke, J. Tamkun, and R.O. Hynes. 1986. Plakoglobin: a protein common to different kinds of intercellular adhering junctions. *Cell*. 46:1063–1073. http://dx.doi.org/10.1016/0092-8674(86)90706-3

Dephoure, N., C. Zhou, J. Villén, S.A. Beausoleil, C.E. Bakalarski, S.J. Elledge, and S.P. Gygi. 2008. A quantitative atlas of mitotic phosphorylation. *Proc. Natl. Acad. Sci. USA*. 105:10762–10767. http://dx.doi.org/10.1073/pnas.0805139105

Ebstensen, R.D., and P.G. Plagemann. 1972. Cytochalasin B: inhibition of glucose and glucosamine transport. *Proc. Natl. Acad. Sci. USA*. 69:1430–1434. http://dx.doi.org/10.1073/pnas.69.6.1430

Elbedour, K., N. Zucker, E. Zalzstein, Y. Barki, and R. Carmi. 1994. Cardiac abnormalities in the Bardet-Biedl syndrome: echocardiographic studies of 22 patients. *Am. J. Med. Genet.* 52:164–169. http://dx.doi.org/10.1002/ajmg.1320520208

Frosk, P., T. Weiler, E. Nylen, T. Sudha, C.R. Greenberg, K. Morgan, T.M. Fujiwara, and K. Wrogemann. 2002. Limb-girdle muscular dystrophy type 2H associated with mutation in TRIM32, a putative E3-ubiquitin-ligase gene. *Am. J. Hum. Genet.* 70:663–672. http://dx.doi.org/10.1086/339083

Glass, D.J. 2005. Skeletal muscle hypertrophy and atrophy signaling pathways. *Int. J. Biochem. Cell Biol.* 37:1974–1984. http://dx.doi.org/10.1016/j.biocel.2005.04.018

Glass, D.J. 2010. PI3 kinase regulation of skeletal muscle hypertrophy and atrophy. *Curr. Top. Microbiol. Immunol.* 346:267–278.

Gomes, M.D., S.H. Lecker, R.T. Jagoe, A. Navon, and A.L. Goldberg. 2001. Atrogin-1, a muscle-specific F-box protein highly expressed during muscle atrophy. *Proc. Natl. Acad. Sci. USA*. 98:14440–14445. http://dx.doi.org/10.1073/pnas.251541198

Gosavi, P., S.T. Kundu, N. Khapare, L. Sehgal, M.S. Karkhanis, and S.N. Dalal. 2011. E-cadherin and plakoglobin recruit plakophilin3 to the cell border to initiate desmosome assembly. *Cell. Mol. Life Sci.* 68:1439–1454. http://dx.doi.org/10.1007/s00018-010-0531-3

Gumbiner, B.M. 1996. Cell adhesion: the molecular basis of tissue architecture and morphogenesis. *Cell*. 84:345–357. http://dx.doi.org/10.1016/S0092-8674(00)81279-9

Gumbiner, B.M. 2005. Regulation of cadherin-mediated adhesion in morphogenesis. *Nat. Rev. Mol. Cell Biol.* 6:622–634. http://dx.doi.org/10.1038/nrm1699

Herren, T., P.A. Gerber, and F. Duru. 2009. Arrhythmogenic right ventricular cardiomyopathy/dysplasia: a not so rare "disease of the desmosome" with multiple clinical presentations. *Clin. Res. Cardiol.* 98:141–158. http://dx.doi.org/10.1007/s00392-009-0751-4

Horn, E.J., A. Albor, Y. Liu, S. El-Hizawi, G.E. Vanderbeek, M. Babcock, G.T. Bowden, H. Hennings, G. Lozano, W.C. Weinberg, and M. Kulesz-Martin. 2004. RING protein Trim32 associated with skin carcinogenesis has anti-apoptotic and E3-ubiquitin ligase properties. *Carcinogenesis*. 25:157–167. http://dx.doi.org/10.1093/carcin/bgh003

Ichimura, T., M. Taoka, I. Shoji, H. Kato, T. Sato, S. Hatakeyama, T. Isobe, and N. Hachiya. 2013. 14-3-3 proteins sequester a pool of soluble TRIM32 ubiquitin ligase to repress autoubiquitylation and cytoplasmic body formation. *J. Cell Sci.* 126:2014–2026. http://dx.doi.org/10.1242/jcs.122069

Jamora, C., and E. Fuchs. 2002. Intercellular adhesion, signalling and the cytoskeleton. *Nat. Cell Biol.* 4:E101–E108. http://dx.doi.org/10.1038/ncb0402-e101

Kano, S., N. Miyajima, S. Fukuda, and S. Hatakeyama. 2008. Tripartite motif protein 32 facilitates cell growth and migration via degradation of Abl-interactor 2. *Cancer Res.* 68:5572–5580. http://dx.doi.org/10.1158/0008-5472.CAN-07-6231

Koch, P.J., and W.W. Franke. 1994. Desmosomal cadherins: another growing multigene family of adhesion molecules. *Curr. Opin. Cell Biol.* 6:682–687. http://dx.doi.org/10.1016/0955-0674(94)90094-9

Kudryashova, E., A. Struyk, E. Mokhonova, S.C. Cannon, and M.J. Spencer. 2011. The common missense mutation D489N in TRIM32 causing limb girdle muscular dystrophy 2H leads to loss of the mutated protein in knock-in mice resulting in a Trim32-null phenotype. *Hum. Mol. Genet.* 20:3925–3932. http://dx.doi.org/10.1093/hmg/ddr311

Kudryashova, E., I. Kramerova, and M.J. Spencer. 2012. Satellite cell senescence underlies myopathy in a mouse model of limb-girdle muscular dystrophy 2H. *J. Clin. Invest.* 122:1764–1776. http://dx.doi.org/10.1172/JCI59581

Kundu, S.T., P. Gosavi, N. Khapare, R. Patel, A.S. Hosing, G.B. Maru, A. Ingle, J.A. Decaprio, and S.N. Dalal. 2008. Plakophilin3 downregulation leads to a decrease in cell adhesion and promotes metastasis. *Int. J. Cancer*. 123:2303–2314. http://dx.doi.org/10.1002/ijc.23797

Lecker, S.H., R.T. Jagoe, A. Gilbert, M. Gomes, V. Baracos, J. Bailey, S.R. Price, W.E. Mitch, and A.L. Goldberg. 2004. Multiple types of skeletal muscle atrophy involve a common program of changes in gene expression. *FASEB J.* 18:39–51. http://dx.doi.org/10.1096/fj.03-0610com

Li, J., D. Swope, N. Raess, L. Cheng, E.J. Muller, and G.L. Radice. 2011. Cardiac tissue-restricted deletion of plakoglobin results in progressive cardiomyopathy and activation of beta-catenin signaling. *Mol. Cell. Biol.* 31:1134–1144. http://dx.doi.org/10.1128/MCB.01025-10

Liu, Y., J.P. Lagowski, S. Gao, J.H. Raymond, C.R. White, and M.F. Kulesz-Martin. 2010. Regulation of the psoriatic chemokine CCL20 by E3 ligases Trim32 and Piasy in keratinocytes. *J. Invest. Dermatol.* 130:1384–1390. http://dx.doi.org/10.1038/jid.2009.416

Locke, M., C.L. Tinsley, M.A. Benson, and D.J. Blake. 2009. TRIM32 is an E3 ubiquitin ligase for dysbindin. *Hum. Mol. Genet.* 18:2344–2358. http://dx.doi.org/10.1093/hmg/ddp167

Mammucari, C., G. Milan, V. Romanello, E. Masiero, R. Rudolf, P. Del Piccolo, S.J. Burden, R. Di Lisi, C. Sandri, J. Zhao, et al. 2007. FoxO3 controls autophagy in skeletal muscle in vivo. *Cell Metab.* 6:458–471. http://dx.doi.org/10.1016/j.cmet.2007.11.001

Näthke, I.S., L. Hinck, J.R. Swedlow, J. Papkoff, and W.J. Nelson. 1994. Defining interactions and distributions of cadherin and catenin complexes in polarized epithelial cells. *J. Cell Biol.* 125:1341–1352. http://dx.doi.org/10.1083/jcb.125.6.1341

Piccirillo, R., and A.L. Goldberg. 2012. The p97/VCP ATPase is critical in muscle atrophy and the accelerated degradation of muscle proteins. *EMBO J.* 31:3334–3350. http://dx.doi.org/10.1038/emboj.2012.178

Ruiz, P., V. Brinkmann, B. Ledermann, M. Behrend, C. Grund, C. Thalhammer, F. Vogel, C. Birchmeier, U. Günthert, W.W. Franke, and W. Birchmeier. 1996. Targeted mutation of plakoglobin in mice reveals essential functions of desmosomes in the embryonic heart. *J. Cell Biol.* 135:215–225. http://dx.doi.org/10.1083/jcb.135.1.215

Sacheck, J.M., A. Ohtsuka, S.C. McLary, and A.L. Goldberg. 2004. IGF-I stimulates muscle growth by suppressing protein breakdown and expression of atrophy-related ubiquitin ligases, atrogin-1 and MuRF1. *Am. J. Physiol. Endocrinol. Metab.* 287:E591–E601. http://dx.doi.org/10.1152/ajpendo.00073.2004

Sandri, M., C. Sandri, A. Gilbert, C. Skurk, E. Calabria, A. Picard, K. Walsh, S. Schiaffino, S.H. Lecker, and A.L. Goldberg. 2004. Foxo transcription factors induce the atrophy-related ubiquitin ligase atrogin-1 and cause skeletal muscle atrophy. *Cell*. 117:399–412. http://dx.doi.org/10.1016/S0092-8674(04)00400-3

Schakman, O., S. Kalista, L. Bertrand, P. Lause, J. Verniers, J.M. Ketelslegers, and J.P. Thissen. 2008. Role of Akt/GSK-3beta/beta-catenin transduction pathway in the muscle anti-atrophy action of insulin-like growth factor-I in glucocorticoid-treated rats. *Endocrinology*. 149:3900–3908. http://dx.doi.org/10.1210/en.2008-0439

Slack, F.J., and G. Ruvkun. 1998. A novel repeat domain that is often associated with RING finger and B-box motifs. *Trends Biochem. Sci.* 23:474–475. http://dx.doi.org/10.1016/S0968-0004(98)01299-7

Smith, E.A., and E. Fuchs. 1998. Defining the interactions between intermediate filaments and desmosomes. *J. Cell Biol.* 141:1229–1241. http://dx.doi.org/10.1083/jcb.141.5.1229

Stitt, T.N., D. Drujan, B.A. Clarke, F. Panaro, Y. Timofeyva, W.O. Kline, M. Gonzalez, G.D. Yancopoulos, and D.J. Glass. 2004. The IGF-1/PI3K/Akt pathway prevents expression of muscle atrophy-induced ubiquitin ligases by inhibiting FOXO transcription factors. *Mol. Cell*. 14:395–403. http://dx.doi.org/10.1016/S1097-2765(04)00211-4

Venkiteswaran, K., K. Xiao, S. Summers, C.C. Calkins, P.A. Vincent, K. Pumiglia, and A.P. Kowalczyk. 2002. Regulation of endothelial barrier function and growth by VE-cadherin, plakoglobin, and beta-catenin. *Am. J. Physiol. Cell Physiol.* 283:C811–C821. http://dx.doi.org/10.1152/ajpcell.00417.2001

Wang, X., Z. Hu, J. Hu, J. Du, and W.E. Mitch. 2006. Insulin resistance accelerates muscle protein degradation: Activation of the ubiquitin-proteasome pathway by defects in muscle cell signaling. *Endocrinology*. 147:4160–4168. http://dx.doi.org/10.1210/en.2006-0251

Winn, R.A., R.M. Bremnes, L. Bemis, W.A. Franklin, Y.E. Miller, C. Cool, and L.E. Heasley. 2002. gamma-Catenin expression is reduced or absent in a subset of human lung cancers and re-expression inhibits transformed cell growth. *Oncogene*. 21:7497–7506. http://dx.doi.org/10.1038/sj.onc.1205963

Woodfield, R.J., M.N. Hodgkin, N. Akhtar, M.A. Morse, K.J. Fuller, K. Saqib, N.T. Thompson, and M.J. Wakelam. 2001. The p85 subunit of phosphoinositide 3-kinase is associated with beta-catenin in the cadherin-based adhesion complex. *Biochem. J.* 360:335–344. http://dx.doi.org/10.1042/0264-6021:3600335

Yin, T., S. Getsios, R. Caldelari, A.P. Kowalczyk, E.J. Müller, J.C. Jones, and K.J. Green. 2005. Plakoglobin suppresses keratinocyte motility through both cell-cell adhesion-dependent and -independent mechanisms. *Proc. Natl. Acad. Sci. USA*. 102:5420–5425. http://dx.doi.org/10.1073/pnas.0501676102

Yokota, T., M. Mishra, H. Akatsu, Y. Tani, T. Miyauchi, T. Yamamoto, K. Kosaka, Y. Nagai, T. Sawada, and K. Heese. 2006. Brain site-specific gene expression analysis in Alzheimer's disease patients. *Eur. J. Clin. Invest.* 36:820–830. http://dx.doi.org/10.1111/j.1365-2362.2006.01722.x

Zhao, J., J.J. Brault, A. Schild, P. Cao, M. Sandri, S. Schiaffino, S.H. Lecker, and A.L. Goldberg. 2007. FoxO3 coordinately activates protein degradation by the autophagic/lysosomal and proteasomal pathways in atrophying muscle cells. *Cell Metab.* 6:472–483. http://dx.doi.org/10.1016/j.cmet.2007.11.004

Zhou, X., J.L. Wang, J. Lu, Y. Song, K.S. Kwak, Q. Jiao, R. Rosenfeld, Q. Chen, T. Boone, W.S. Simonet, et al. 2010. Reversal of cancer cachexia and muscle wasting by ActRIIB antagonism leads to prolonged survival. *Cell*. 142:531–543. http://dx.doi.org/10.1016/j.cell.2010.07.011

Zhurinsky, J., M. Shtutman, and A. Ben-Ze'ev. 2000a. Differential mechanisms of LEF/TCF family-dependent transcriptional activation by beta-catenin and plakoglobin. *Mol. Cell. Biol.* 20:4238–4252. http://dx.doi.org/10.1128/MCB.20.12.4238-4252.2000

Zhurinsky, J., M. Shtutman, and A. Ben-Ze'ev. 2000b. Plakoglobin and beta-catenin: protein interactions, regulation and biological roles. *J. Cell Sci.* 113:3127–3139.